

## 石墨烯负载的氧配位钴单原子稳定金属锂负极

石浩东<sup>1,2,3</sup>, 李亚光<sup>1,2</sup>, 路鹏飞<sup>1,2</sup>, 吴忠帅<sup>1,2,\*</sup>

<sup>1</sup> 中国科学院大连化学物理研究所, 催化基础国家重点实验室, 辽宁 大连 116023

<sup>2</sup> 中国科学院洁净能源创新研究院, 辽宁 大连 116023

<sup>3</sup> 中国科学院大学, 北京 100049

## Single-Atom Cobalt Coordinated to Oxygen Sites on Graphene for Stable Lithium Metal Anodes

Haodong Shi<sup>1,2,3</sup>, Yaguang Li<sup>1,2</sup>, Pengfei Lu<sup>1,2</sup>, Zhong-Shuai Wu<sup>1,2,\*</sup>

<sup>1</sup> State Key Laboratory of Catalysis, Dalian Institute of Chemical Physics, Chinese Academy of Sciences, Dalian 116023, Liaoning Province, China.

<sup>2</sup> Dalian National Laboratory for Clean Energy, Chinese Academy of Sciences, Dalian 116023, Liaoning Province, China.

<sup>3</sup> University of Chinese Academy of Sciences, Beijing 100049, China.

\*Corresponding author. Email: wuzs@dicp.ac.cn; Tel.: +86-411-82463036.

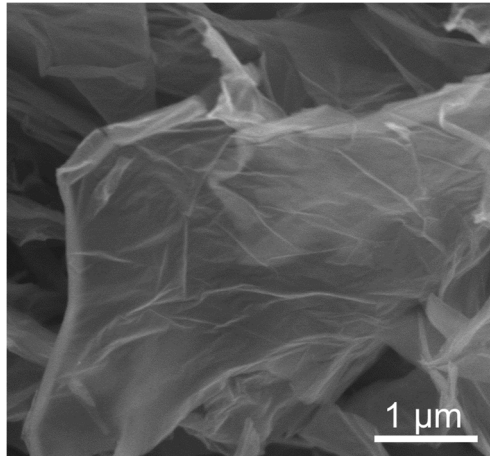


Fig. S1 SEM image of Co-O-G SA.

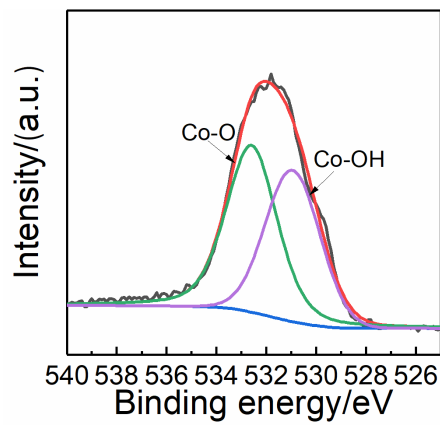


Fig. S2 High resolution O 1s XPS spectrum of Co-O-G SA.

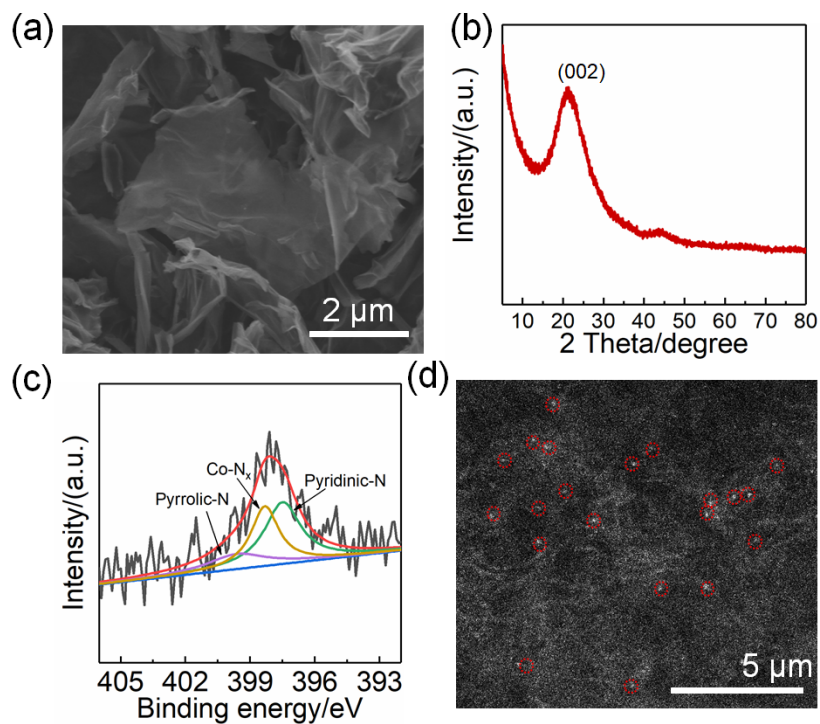


Fig. S3 Characterizations of the as-prepared Co-N-G SA. (a) SEM image, and (b) XRD pattern of Co-N-G SA. (c) High resolution N 1s XPS spectrum of Co-N-G SA.

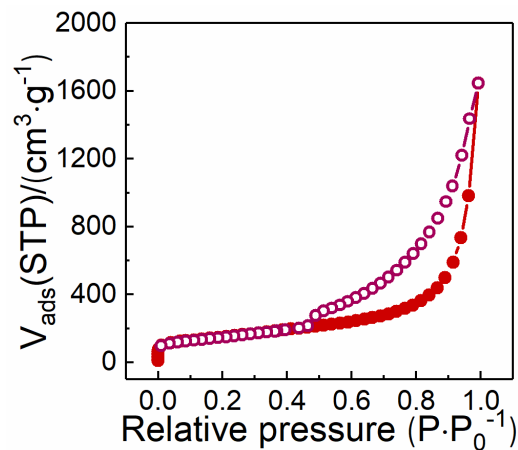


Fig. S4 Nitrogen adsorption-desorption isotherm of Co-N-G SA.

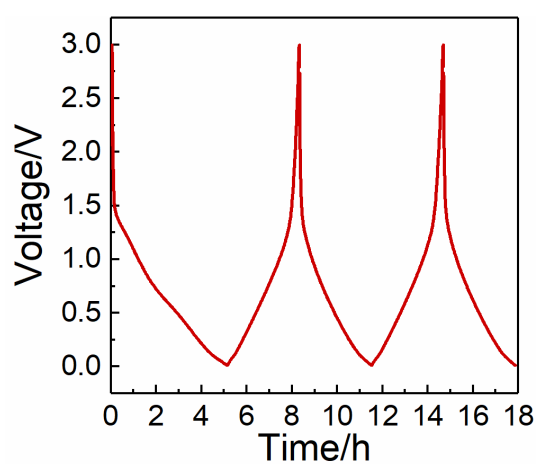


Fig. S5 Typical voltage profiles of Co-O-G SA electrode obtained at the initial 3 cycles. The first 3 cycles at 0.01–3 V was set to Li intercalation and stabilize the SEI film.

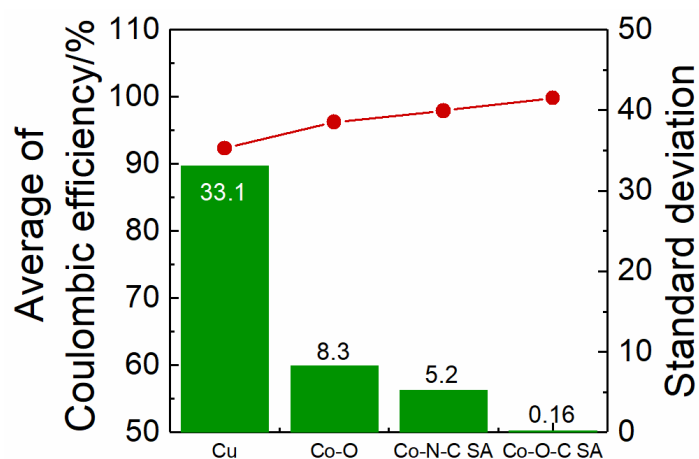


Fig. S6 The average Coulombic efficiencies and their corresponding standard deviations of Co-O-G SA, Co-N-G SA, G-O and Cu electrodes with Li deposition amount of  $0.5 \text{ mAh cm}^{-2}$  at  $0.5 \text{ mA}\cdot\text{cm}^{-2}$ .

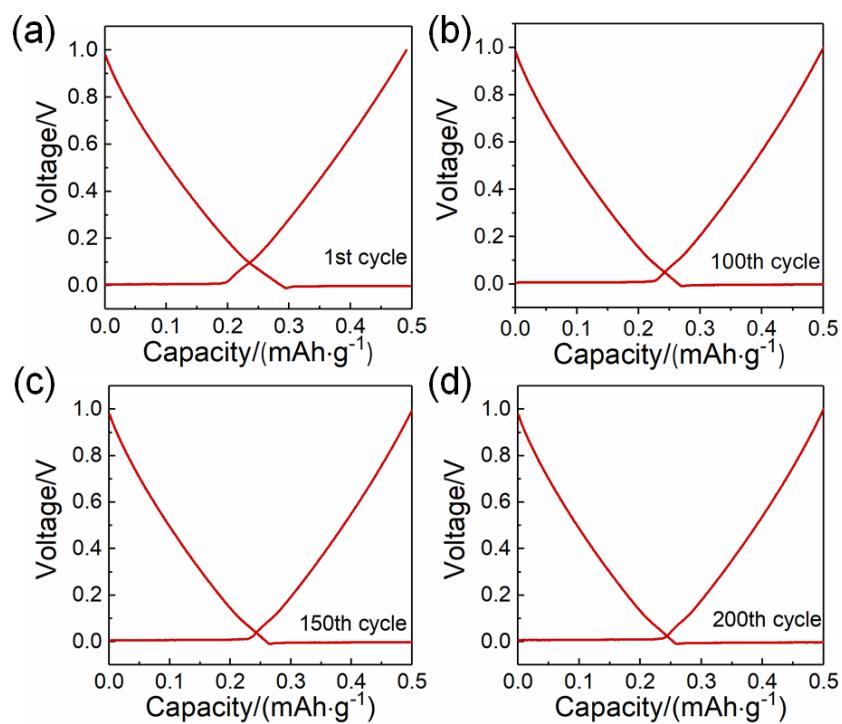


Fig. S7 Voltage profiles of Co-O-G SA electrodes tested at different cycles. Planting 0.5 mAh·cm<sup>-2</sup> of Li at a current density of 0.5 mA·cm<sup>-2</sup> at (a) 1st cycle, (b) 100th cycle, (c) 150th cycle, and (d) 200th cycle.

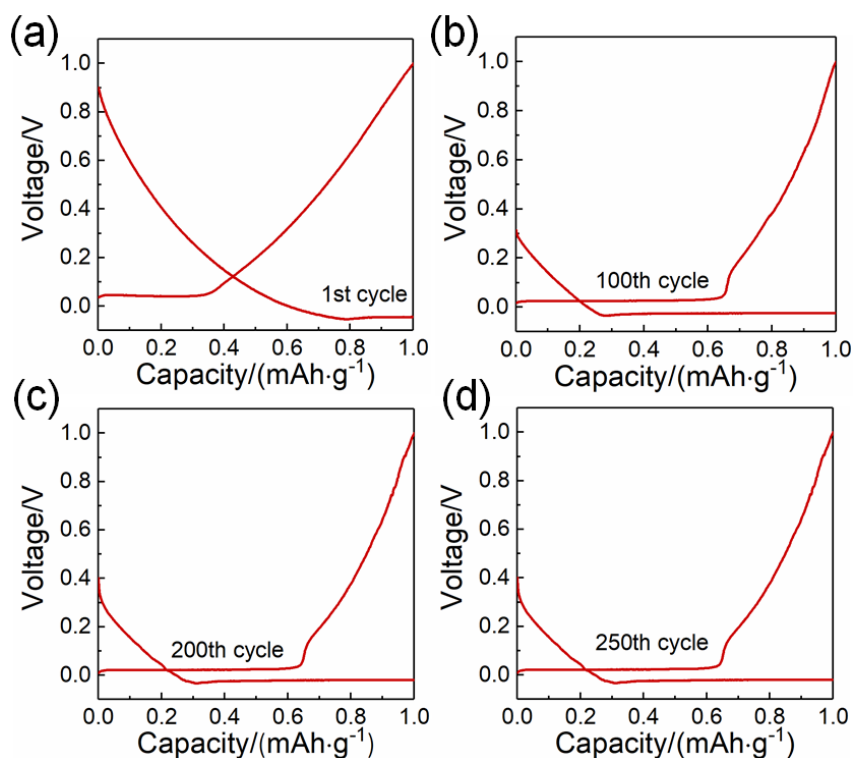


Fig. S8 Voltage profiles of Co-O-G SA electrodes tested at different cycles. Planting 1 mAh cm<sup>-2</sup> of Li at a current density of 1 mA·cm<sup>-2</sup> at (a) 1st cycle, (b) 100th cycle, (c) 200th cycle, and (d) 250th cycle.

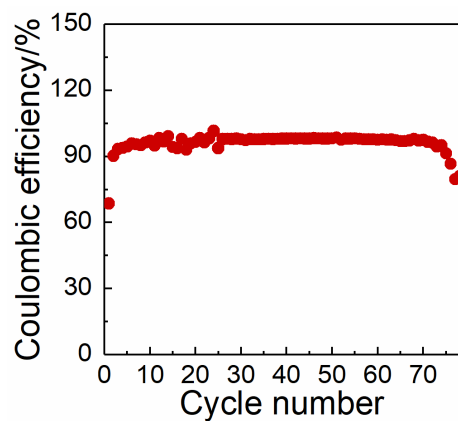


Fig. S9 The Coulombic efficiency of Co-O-G SA electrode obtained at  $1 \text{ mA}\cdot\text{cm}^{-2}$  with  $1 \text{ mAh cm}^{-2}$  with a low mass loading of  $0.2 \text{ mg cm}^{-2}$ .

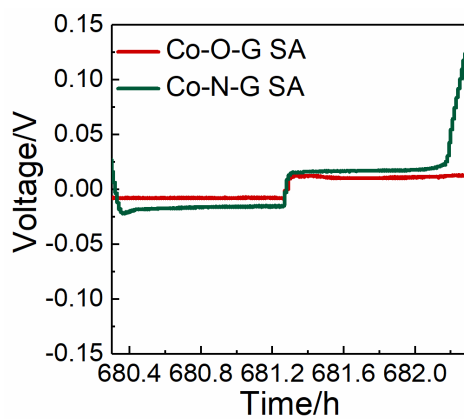


Fig. S10 Detailed voltage profiles of Co-O-G SA/Li and Co-N-G SA/Li symmetric cells at current density of  $1 \text{ mA}\cdot\text{cm}^{-2}$  under stripping/plating capacity of  $1 \text{ mAh}\cdot\text{cm}^{-2}$ .

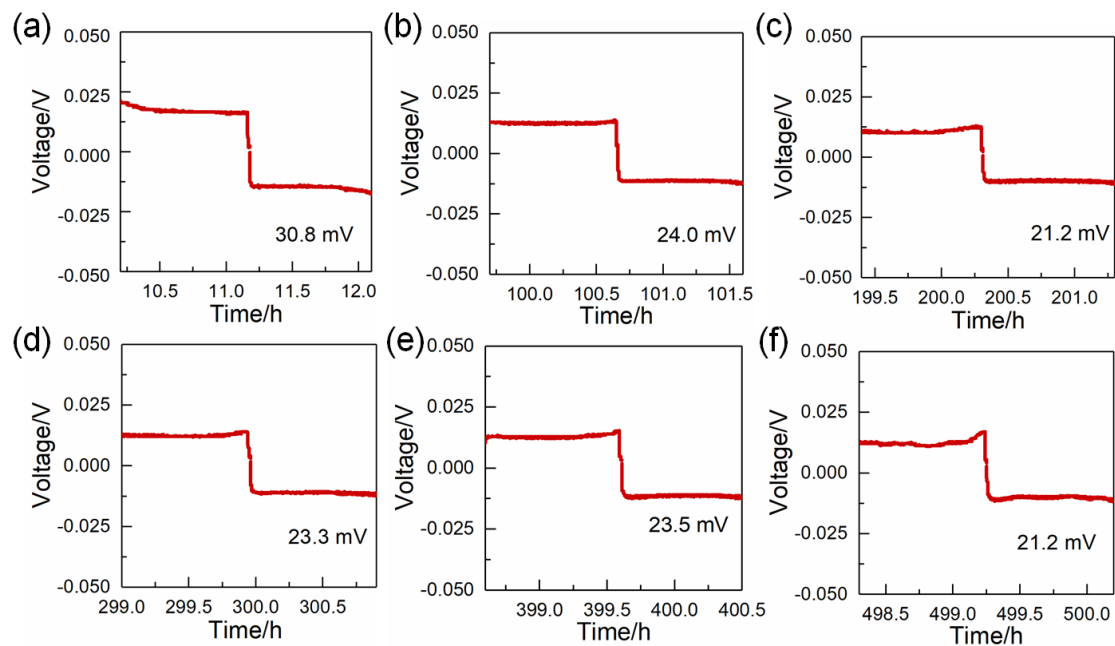


Fig. S11 Detailed voltage profiles of Co-O-G SA/Li symmetric cells at current density of  $3 \text{ mA}\cdot\text{cm}^{-2}$  under stripping/plating capacity of  $3 \text{ mAh}\cdot\text{cm}^{-2}$ .

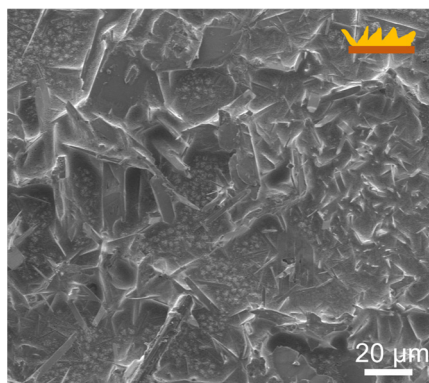


Fig. S12 Top view SEM image of Co-N-G SA electrode at the stage of plating Li with capacity of  $1 \text{ mAh}\cdot\text{cm}^{-2}$ .

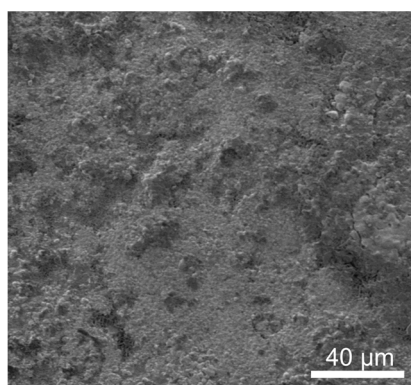


Fig. S13 Top-view SEM image of Co-O-G SA electrode after 250 cycles with a deposition capacity of  $1 \text{ mAh}\cdot\text{cm}^{-2}$  at  $1 \text{ mA}\cdot\text{cm}^{-2}$ .

Table S1 EXAFS fitting parameters of Co-O-G SA.

Sample	Path	CN	R/(Å)	$\sigma^2/(10^{-3} \text{ Å}^2)$	$\Delta E_0(\text{eV})$	R-factor
Co-O-G	Co-O	$3.9 \pm 0.2$	$2.06 \pm 0.01$	$6.0 \pm 0.6$	$1.7 \pm 0.4$	0.004
	Co-OH	$2.0 \pm 0.2$	$2.11 \pm 0.01$			

Table S2 Electrochemical performance comparison with the recent publications in single atom-based Li anode.

Materials	Current density/( $\text{mA}\cdot\text{cm}^{-2}$ )	Areal capacity/( $\text{mAh}\cdot\text{cm}^{-2}$ )	Cycle time	Ref.
single-atom Zn	1	2	~1050 h	1
S-doped G	1	2	240 h	2
Zn-MXene	1	1	1200 h	3
SANi-NG	1	2	560 h	4
CoN <sub>x</sub> -doped graphene	10	2	800 h	5
<b>Co-O-G SA</b>	<b>8</b>	<b>8</b>	<b>1300 h</b>	<b>This work</b>

G: graphene; SANi-NG: Atomically dispersed Ni on N doped graphene.

## References

- (1) Xu, K.; Zhu, M.; Wu, X.; Liang, J.; Liu, Y.; Zhang, T.; Zhu, Y.; Qian, Y. *Energy Storage Mater.* **2019**, *23*, 587. doi:10.1016/j.ensm.2019.03.025
- (2) Wang, T.; Zhai, P.; Legut, D.; Wang, L.; Liu, X.; Li, B.; Dong, C.; Fan, Y.; Gong, Y.; Zhang, Q. *Adv. Energy Mater.* **2019**, *9*, 1804000. doi:10.1002/aenm.201804000
- (3) Gu, J.; Zhu, Q.; Shi, Y.; Chen, H.; Zhang, D.; Du, Z.; Yang, S. *ACS Nano* **2020**, *14*, 891. doi: 10.1021/acsnano.9b08141
- (4) Zhai, P.; Wang, T.; Yang, W.; Cui, S.; Zhang, P.; Nie, A.; Zhang, Q.; Gong, Y. *Adv. Energy Mater.* **2019**, *9*, 1804019. doi: 10.1002/aenm.201804019
- (5) Liu, H.; Chen, X.; Cheng, X.-B.; Li, B.-Q.; Zhang, R.; Wang, B.; Chen, X.; Zhang, Q. *Small Methods* **2019**, *3*, 1800354. doi: 10.1002/smtd.201800354